ARTICLE

Self-Assembly of Chemically Engineered Hydrophilic Dextran into Microscopic Tubules

Guoming Sun[†,§] and Chih-Chang Chu[†,‡,*]

[†]Fiber and Polymer Science Program, Department of Fiber Science & Apparel Design, Cornell University, Ithaca, New York 14853-4401, and [‡]Department of Biomedical Engineering, Cornell University, Ithaca, New York 14853-5201. [§]Present address: Department of Chemical and Biomolecular Engineering, Johns Hopkins University, 3400 N Charles Street, Baltimore, Maryland 21218.

ABSTRACT Although macromolecular self-assemblies are mostly fabricated from amphiphilic copolymers, here we report a tubular structure self-assembled solely from hydrophilic dextran-derived homopolymers *via* electrostatic interaction. To obtain tubular structures, we prepared two oppositely charged dextran derivatives by incorporating 2-bromoethylamine (Dex-BH) and chloroacetic acid (Dex-CA) into dextran, and their structures were confirmed using Fourier transform infrared spectroscopy. The two oppositely charged dextran derivatives self-assembled into microsize tubules when mixed in a pH 4.0 buffer solution. The tubular self-assemblies were sensitive to both pH and salt concentrations. Scanning electron microscopy and light microscopy confirmed that the tubules have hollow structures up to 100 μm long with a diameter between 600 nm and 2 μm. The X-ray study did not reveal any ordered molecular organization. This paper explores the mechanism of the tubule self-assembly and suggests a model.

KEYWORDS: self-assembly · dextran · tubule · polysaccharide · hydrophilic

Molecules usually work together to perform particular functions; the molecular engineering of functional materials is generally achieved by supramolecular self-assembly. Many biological materials with different morphologies, such as tubules, vesicles, and hydrogels, have been fabricated using bottom-up self-assembly.[1−4] These macromolecular assemblies were generated predominantly from DNA, peptides, proteins, lipids, copolymers, and dendrimers; they play a far more crucial role in governing the structures and functions of the entire body than any individual molecule. These assemblies are effective carriers or scaffolds for controlled release, cell culture, and tissue engineering[5−8] and also have potential use in other applications.[1,9] Among these assemblies, tubules are of special interest for both basic research and applications due to their unique structural features.[10,11]

Most assembled tubular structures are formed from amphiphilic molecules, including lipids,[10] macrocylic molecules,[11] copolymers,[2,12] and peptides.[13,14] Amphiphilic oligomers, including peptides and other small molecules, will self-assemble into tubules in an aqueous solution due to their hydrophobic interactions, which drive the nonpolar region of each molecule away from the water molecules and toward one another.[15] Similar to oligomers, these self-assembling tubules derived from block or alternating copolymers are normally driven by the aggregation of the hydrophobic regions. Eisenberg *et al.*[16] prepared bilayer tubular structures from diblock polystyrene-*b*-poly(ethylene oxide) (PS-*b*-PEO) copolymer in a mixture of DMF and water. Similarly, Grumelard *et al.*[17] obtained nanotubes from triblock copolymer, that is, poly(2-methyloxazoline-block-dimethylsiloxaneblock-2-methyloxazoline) (PMOXA-*b*-PDMS-*b*-PMOXA) in chloroform, where hydrophobic PDMS formed the wall while hydrophilic PMOXA formed the inner and outer layers.

Other tubular structures are self-assembled through different association mechanisms. Raez *et al.*[12] reported nanotube self-assembly derived from the crystallization of poly(ferrocenylsilane-siloxane) diblock copolymers, in which the crystalline regions facilitated the wall formation of nanotubes. However, the multiwall macrotubes self-assembled from multiarm block copolymers were induced by microphase separation and further driven by the formation of hydrogen bonds.[2] Ghadiri *et al.*[18] found nanotubes that were self-assembled by stacking cyclic peptides through backbone−backbone intermolecular hydrogen bonding. Molecular chirality also plays an important role in the self-assembly of tubule structures.[19,20] The packing of chiral molecules usually causes an intrinsic bending force, thus driving the chiral membranes to fold into tubes. Another strategy

*Address correspondence to cc62@cornell.edu.

Received for review October 22, 2008 and accepted April 20, 2009.

Published online April 23, 2009.
10.1021/nn800704q CCC: $40.75

for tube self-assembly was achieved by manipulating the interactions between biological polyelectrolyte and oppositely charged membranes. Wong *et al.* prepared ribbon-like tubules self-assembled from cytoskeletal filamentous actin (F-actin) and cationic lipid membranes.[21] According to Wong *et al.*, G-actin self-assembled into F-actin filaments followed by the spontaneous formation of 2D crystal layer F-actin; the F-actin coated membranes would then fold into ribbon-like tubules. Although each type of tubular structure has been explored, the mechanism of tube self-assembly remains poorly understood, and the self-assembly of tubular structures from hydrophilic homopolymers has not been reported in the literature. Unveiling the mechanisms of various self-assemblies would offer significant directions for fabricating novel materials.

Herein, we report a tubular self-assembly from hydrophilic polymers. To make the tubular structure, we synthesized two hydrophilic polymers: dextran-bromoethylamine hydrobromide (Dex-BH) and dextran-chloroacetic acid (Dex-CA), and their structures were confirmed using Fourier transform infrared spectroscopy (FTIR). When Dex-BH and Dex-CA were mixed in pH 4.0 buffer solution, we discovered tubular structures under different conditions. A few environmental factors, such as pH and salt concentration, were investigated to determine their effects on tube formations. Scanning electron microscopy (SEM), light microscopy (LM), dynamic light scattering (DLS) and X-ray were used to examine the self-assembled tubular objects. This paper concludes with a model of the tubular self-assembly.

RESULTS AND DISCUSSION

Dextran has chemically active hydroxyl groups that can be chemically engineered into desirable derivatives. The synthesis and characterization of Dex-BH and Dex-CA is shown in Figure 1. The absorption at 1650 cm^{-1} (peak 1) in the dextran (MW 6000, spectrum A) was due to the presence of trace amounts of adsorbed water.[22] The absorption at 1635 cm^{-1} (peak 2) in spectrum B (Dex-BH) is the N−H scissor bending vibration of the amine group, which indicates that the amine group has been grafted into dextran (Dex-BH). In spectrum C (Dex-CA), the band at 1747 cm^{-1} (peak 3) is caused by the C═O stretching vibration, an indication of a successful incorporation of the -COOH group into dextran (Dex-CA). Spectrum D is the self-assembly from the Dex-BH (2.5 mg/mL) and Dex-CA (2.5 mg/mL) precursor solutions. The absorptions at 2485 cm^{-1} (peak 4) and 1950 cm^{-1} (peak 5) are attributed to the N−H stretching vibrations of protonated amine groups (NH_3^+), while the bands at 1675 cm^{-1} (peak 6) and 1485 cm^{-1} (peak 8) are attributed to the N−H asymmetric and symmetric bending of protonated amine groups (NH_3^+). The bands at 1675 cm^{-1} (peak 7) and 1485 cm^{-1} (peak 9) are attributed to the asymmetric

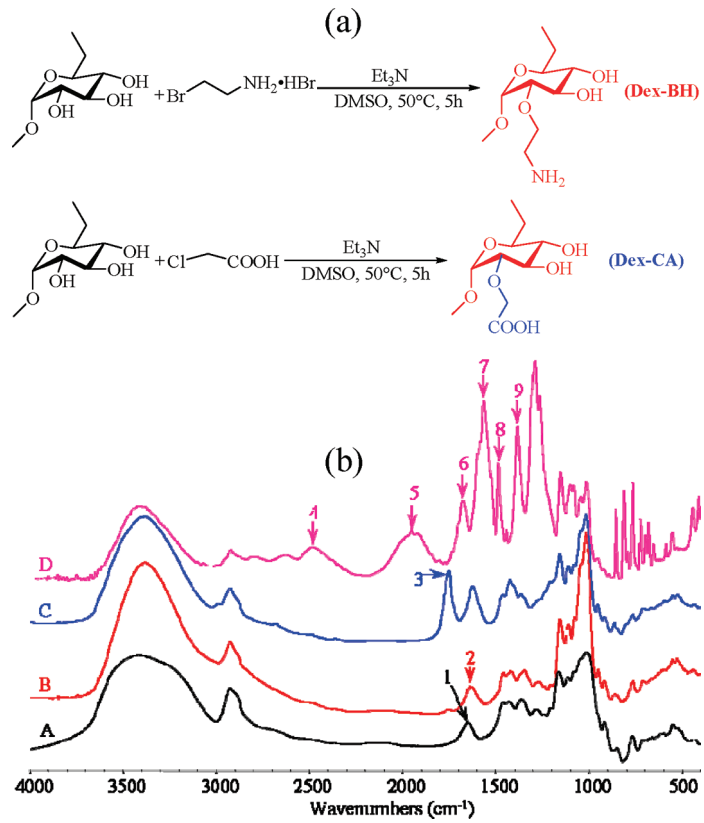

Figure 1. (a) Synthesis and characterization of dextran derivatives Dex-BH and Dex-CA. (b) FTIR spectra of (A) Dextran, (B) Dex-BH, (C) Dex-CA, (D) self-assembly: (1) 1653, (2) 1635, (3) 1749, (4) 2485, (5) 1950, (6) 1675, (7) 1564, (8) 1485, (9) 1384 cm^{-1}.

and symmetric stretching vibrations of the carboxylate anion (COO^-). These FTIR results indicate that the carboxyl groups of Dex-CA are dissociated into COO^- groups, which in turn form a polyelectrolyte complex with protonated amino groups of Dex-BH through electrostatic interaction. Similar interactions between chitosan and poly(acrylic acid) have been reported.[23]

The tubular structure was initially discovered in the freeze-dried solution by scanning electron microscope (SEM). Figure 2Ai shows that the cylindrical aggregates are randomly oriented and their length range from around 4−10 μm. These self-assembled microtubes have a hollow structure.

To confirm the tubular structure observed from the freeze-dried method, the self-assembled aggregate was also air-dried and examined by SEM. Figure 2Aii shows that the tubules obtained by the air-dried method are regularly arrayed and over 100 μm in length, which are much longer than those obtained by the freeze-dried method. This difference may suggest that the freeze-drying process disturbs or even disrupts the array of tubular self-assembling, thus leading to much shorter and randomly dispersed tubes (Figure 2Ai). The end view of the tubules, especially the arrow pointed tubules and their enlarged area clearly shows open-ended structures (Figure 2Aiii), although they protrude irregularly. The SEM images in Figure 2 panels Aii and Aiii sug-

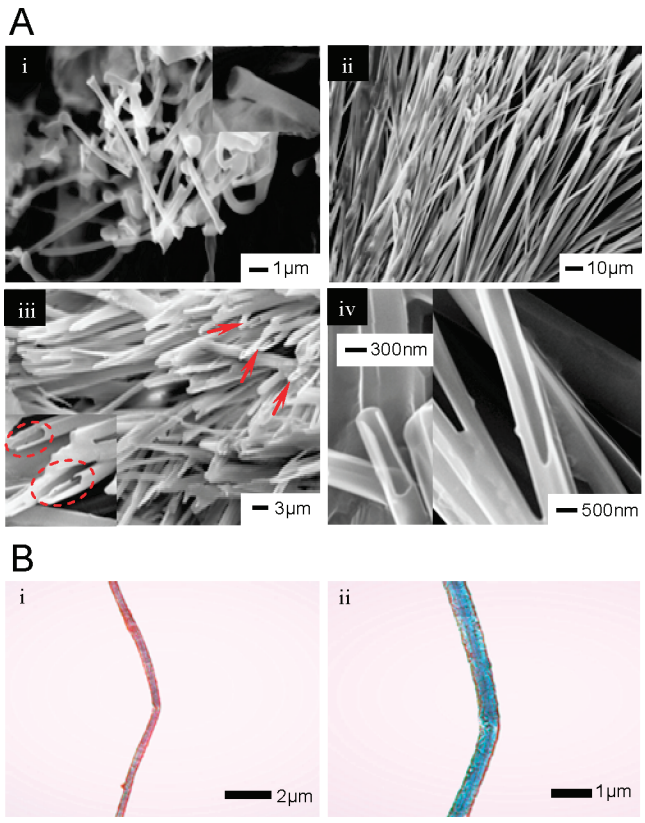

Figure 2. Self-assembly of tubule structures observed at different conditions. (A) SEM micrographs of self-assembly tubules: (i) freeze-dried tubules; (ii) the longitudinal view of air-dried tubules; (iii) the end view of air-dried tubules; (iv) higher magnification of open tubules. (B) Light microscopy images of the assembled tubules in an aqueous state.

gest that these tubes grew individually during the self-assembling process; otherwise, they would have had similar structures. A higher magnification image of the end tubules (Figure 2Aiv) further confirms the hollow structure of these tubes with diameter ranging from 500 nm to 1 mm, indicating the tubules grow in both longitudinal and transverse directions simultaneously, but not proportionally. However, Yan *et al*. showed that the diameter of tubules self-assembled from multi-armed copolymers could reach 1.5 mm.[2] Although SEM images reveal that the tubules are hollow, it is difficult to elucidate how these tubes were formed based on the SEM morphology information alone.

Although the SEM images under both freeze-dried and air-dried conditions reveal that these self-assemblies are hollow tubules, some structures may have been disrupted during the drying process. To find out how the assemblies were formed, it is important to evaluate the assembly morphology under an undisturbed aqueous condition. Figure 2B shows the self-assembling morphology under polarized light microscopy. The image at low magnification (Figure 2Bi) displays only a cylinder structure, but a closer look under a higher magnification (Figure 2Bii) reveals a tubular lumen structure, suggesting the tubules are hollow. This result is consistent with the findings obtained from both air- and freeze-dried self-assemblies.

The self-assembling morphology by both SEM and light microscopy clearly reveals that the assembly has a tubular structure. Many models have been proposed to explain how tubular self-assembly occurs.[2,12,13,18] It is recognized that most self-assembling tubules from either small amphiphilic molecules (*e.g.*, lipid) or block/alternating copolymers (*e.g.*, PMOXA-*b*-PDMS-*b*-PMOXA[17]) are driven by the aggregation of hydrophobic regions. Such models can easily explain the tubules self-assembled from amphiphilic small molecules, oligomers, or macromers. However, they cannot explain tube assemblies from polysaccharide-based hydrophilic polymers. Unveiling how tubules are self-assembled from hydrophilic polymers like Dex-CA and Dex-BH would provide new insight on the self-assembly of polymers.

The protonated amine group in Dex-BH and the dissociated carboxyl group in Dex-CA only interact and self-assemble in an appropriate pH environment; we thus expect the pH value of the medium to play a key role in this polyvalent self-assembly system. The effect of pH on the self-assembly morphology of our Dex-BH/Dex-CA system is shown in Figure 3. At pH 3.0, the amine groups became highly protonated and strongly interacted with the dissociated carboxyl groups, forming a compact aggregation structure (Figure 3a). At pH 4.0, they self-assembled into neat tube constructions (Figure 3b), suggesting that this pH value provides a favorable environment for this assembling system. As the pH value increased to 5.0 (Figure 3c), the interaction was not strong enough to integrate the two precursors; thus, they formed relatively thicker tube-like structures. At pH 7.0 (Figure 3d), the self-assembled microtubular structure was completely lost; only sheetlike structures without any distinctive morphology formed, indicating that the two precursors were unable to self-assemble under such conditions.

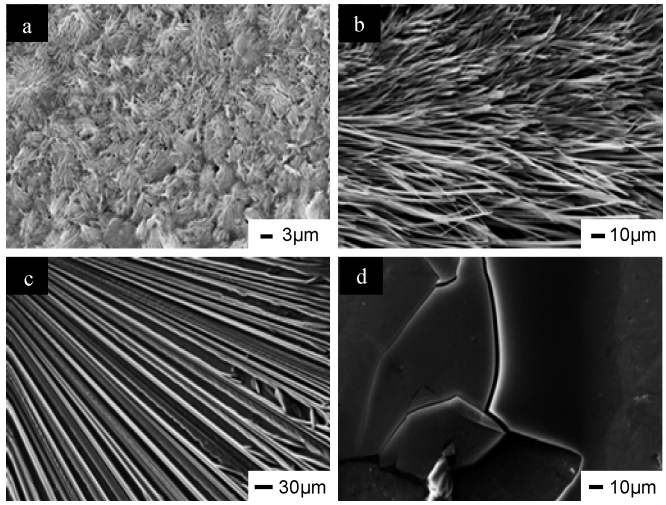

Figure 3. pH effect on the morphology of self-assembly: (a) pH 3.0; (b) pH 4.0; (c) pH 5.0; (d) pH 7.0.

In a lower pH environment, the amine group ($pK_a \approx 10.0$) could become fully protonated (*i.e.*, positively charged), which provides ample binding sites in Dex-BH for the negatively charged carboxyl groups ($pK_a \approx 3.0$) in Dex-CA. However, at higher pH values, the amine groups are likely to exhibit a combination of protonated and deprotonated amine groups. However, the amine groups become less protonated at neutral or higher pH than at lower pH (*e.g.*, pH 4.0), while most amine groups remain deprotonated at pH 7.0. Therefore, the interactions between the protonated amine and deprotonated carboxyl acid groups are not strong enough to drive them into any structural assemblies, though carboxyl acid groups can be fully deprotonated. Therefore, the tubular structures are lost at pH 7.0. In other words, the interaction between the protonated amine groups and the dissociated carboxyl groups is stronger at low pH values than at higher values. This indicates that the self-assembly system requires a delicate balance of intermolecular forces. Matsui *et al*. also found that pH had an effect on the tubule self-assembly of heptane bolaamphiphile.[24] According to their study, the heptane bolaamphiphile could assemble into tubule structures at pH 4.0 but only assembled into helical ribbons at pH 8.0. Meanwhile, Hu *et al*. also found a pH dependence on the formation of nanoparticles in their chitosan-poly(acrylic acid) dramatic system, in which the particle size increased from 400 to 625 nm when the pH increased from 5.8 to 7.4, whereas the nanoparticles were completely destroyed at higher pH (pH $>$ 9.0).[23]

Any chemical species that can interact with amine or carboxyl groups will certainly affect this self-assembly. Because salt contents can theoretically interact with amine or carboxyl groups, they were expected to weaken the intermolecular interactions of the two dextran-based precursors by reducing the direct contact between amine and carboxyl groups. Because the pH study demonstrated that the best tubular structures self-assembled at pH 4.0, this value was used to examine the salt effect.

Figure 4 shows the self-assemblies under different salt concentrations at pH 4.0. Again, the tubular structures were formed without adding any salt (Figure 4a). However, in the 0.01 M NaCl solution, only short nanotube structures of about 600 nm diameter were formed (Figure 4b). In the 0.03 M NaCl solution, a few ring structures formed (Figure 4c). No other structures formed in 0.06 M and higher NaCl solutions (Figure 4d). The addition of salt obviously weakened the macromolecular interactions between Dex-BH (2.5 mg/mL) and Dex-CA (2.5 mg/mL) precursors, as reflected in a slower rate of tube formation process. During normal tube self-assembly without salt, the tubes formed quickly in the early stage, and the tube formation continued without interruption. The addition of salt slowed down the rate of self-assembly. With a lower salt concentration (0.01 M), the salt ions only interacted with part of the carboxyl or amine groups, and thus delayed the rate of tube formation only slightly. However, when the salt concentration increased to 0.03 M (Figure 4c), the rate slowed significantly. The morphological data in Figure 4 suggest that when the dextran-based precursors were mixed, they first formed nanobead-like polyvalent aggregates, which then assembled into a 2D ring structure and grew into 3D tubes.

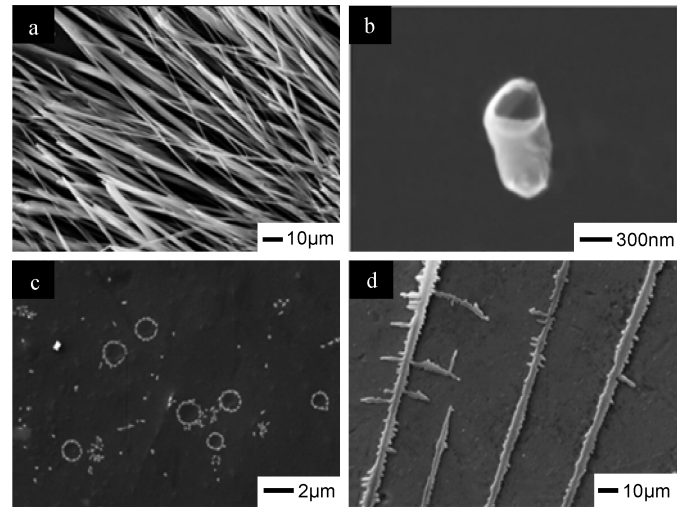

Figure 4. Morphology change induced by salt concentration: (a) tubules assembled in pH 4.0 solution; (b) short tubule formed in a 0.01 M NaCl pH 4.0 solution; (c) rings formed in a 0.03 M NaCl pH 4.0 solution; (d) in a 0.06 M NaCl pH 4.0 solution.

To determine whether there were any ordered structures within the assembly, wide-angle X-ray diffraction was conducted (Figure 5). The X-ray data show that pure dextran has crystalline structures, but its derivatives and their self-assembled aggregates show no signs of crystalline structure. This indicates that no ordered structures formed within the Dex-BH/Dex-CA self-assembled aggregates, and the tube structure was not regulated by the ordered molecular arrangement.

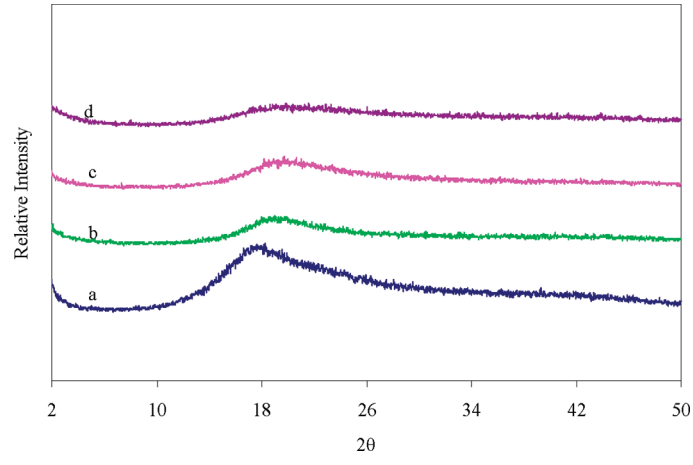

Figure 5. X-ray diffraction pattern of (a) Dextran; (b) Dex-BH; (c) Dex-CA; (d) assembly. This X-ray pattern indicates there is no ordered molecular structures formed during this self-assembly.

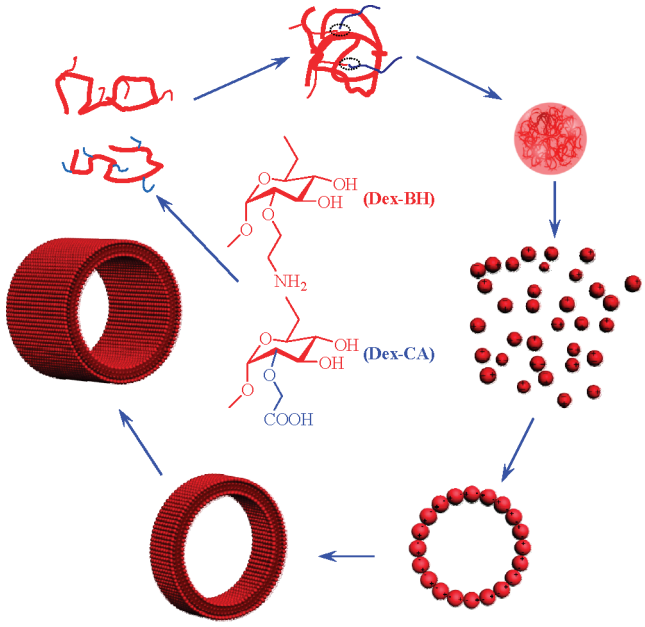

Figure 6. Proposed self-assembly of tubule structures. When mixed, Dex-BH and Dex-CA first form polyvalent tiny beadlike aggregates, which have many positive and negative charges. These tiny beadlike aggregates then lined up to form circles due to the alternating negative and positive charges of adjacent aggregates. These ring structures simultaneously direct the growth of the tubule self-assembly in both longitudinal and transverse directions.

This suggests that the tube structure could be built from randomly coiled dextran-derived macromolecules.

On the basis of the above data and the characteristics of dextran polymer precursors, the mechanism of tube self-assembly is suggested along with a proposed model (Figure 6). Unlike small molecules, which are amphiphilic and can form ordered aggregates *via* simple molecular interactions, their tubular structures can be explained using the bilayer model. Polymeric tubes self-assembled from amphiphilic di- or triblock polymers can also be understood using similar models based on hydrophilic−hydrophobic interactions.[16,17] In the case of dextran-based polymers in this study, however, Dex-BH and Dex-CA are hydrophilic polymers, so their self-assembly follows different mechanisms.

Macromolecules tend to form random coils in solutions. When mixed, the two dextran-based macromolecules first form polyvalent tiny beadlike aggregates, which have many positive and negative charges. These tiny beadlike aggregates could then line up to form circles, which may partially be driven by the electrostatic forces of adjacent aggregates. However, how these ring structures are formed is not clear and beyond the scope of our current work. If the tiny beadlike aggregates do not have appropriate charges or size, they may not participate in the ring formation nor give rise to different ring sizes. These ring structures simultaneously direct the growth of the tubule self-assembly in both longitudinal and transverse directions, and different ring structures could thus lead to a variety of tubule structures.

We can also borrow the ABA triblock copolymer model[17] to explain the tubule structure. Because both Dex-BH and Dex-CA are hydrophilic, the inner and outer layers will be hydrophilic no matter how the molecules are assembled. In this triblock copolymer model, the wall is formed *via* hydrophobic forces, while the wall in our study is formed *via* electrostatic forces.

To test the rationale of this proposed model, we measured the self-assembly size as a function of time using dynamic light scattering (DLS). To monitor the assembly size change over time, the Dex-BH and Dex-CA mixed solution were scanned by DLS at predetermined time intervals; the collected data is shown in Figure 7. According to the published data,[25] the diameter of dextran (6-kD) molecule should be between 4 and 6 nm, so the small peak around 4∼8 nm is attributed to dextran-derived macromolecules. A strong peak was located around 300∼700 nm; the intensity of the peak decreased over time, but the peak became wider. We are not sure what caused the peaks, but according to the above data, they might be attributed to the beadlike or ringlike self-assembled aggregates. During the first hour, there was a middle intensity peak at approximate 2.5−3.5 μm; this peak was not observed after 2 h, indicating that intermediate structures formed during this time. This finding is consistent with our experimental observation that all tubes reported were obtained after 2 h. As result, the DLS data support our proposed model.

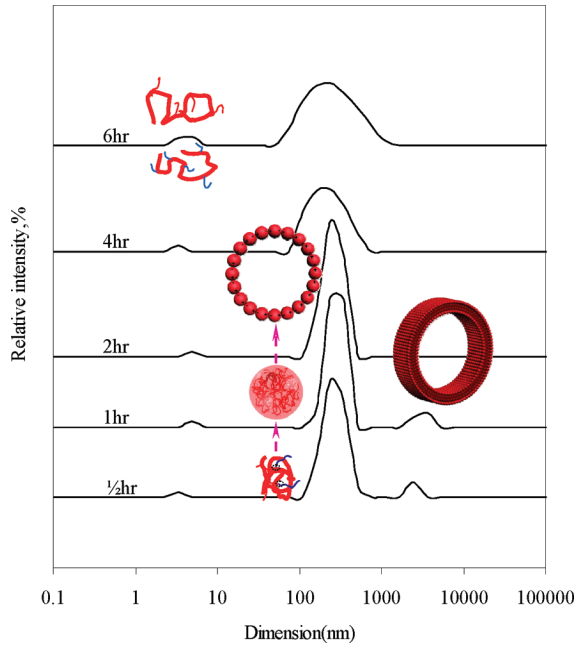

Figure 7. DLS study on Dex-BH/Dex-CA assembly. This result suggests that individual molecules as well as intermediate aggregates coexit in the system.

A full scale scan of the solution at 2 h showed a peak around 100 μm, which might correlate with the length of the tubes. However, as the maximum DLS resolution is only several micrometers long, the 100 μm

peak location from this equipment is not expected to be accurate; thus, this peak is not shown in Figure 7. It is worth noting that tube assembly is a continuous process. The separate peaks in the figure represent different stages of tube assembly.

CONCLUSION

In summary, dextran was chemically modified into Dex-BH and Dex-CA, and their chemical structures were confirmed by FTIR. These two oppositely charged Dex-BH and Dex-CA successfully self-assembled into a tubular structure. Their morphology was observed under freeze- and air-dried conditions as well as in an aqueous solution. The tubule self-assembled *via* electrostatic interaction, but the extent of tube assembly depends on pH value and salt concentration. We suggested that the dextran-based polymers first interact with each other to form tiny beadlike aggregates, which then arrange into circles through electrostatic interactions. After such ring structures form, they grow in both transverse and longitudinal directions until tubes form. Although this tubule model provides a complementary assembly mechanism to what has been proposed, it still needs further investigation to confirm its validity. The tubules may have a potential use as cellular-specific drug carriers because of easy incorporation of different targeting groups into dextran.

EXPERIMENTAL SECTION

Materials. Dextran (MW 6,000) was purchased from Sigma Chemical Company (St. Louis, MO) and dried in a vacuum oven for 24 h at 50 °C before use. Dimethyl sulfoxide (DMSO), triethylamine, 2-bromoethylamine hydrobromide (BEAHB), and chloroacetic acid (CA), were purchased from Aldrich Chemical Co. (Milwaukee, WI). BEAHB and CA were dried in a vacuum oven for 24 h at room temperature before use. Isopropyl alcohol was purchased from J. T. Baker (Philipsburg, NJ). The pH 4.0 buffer solution (biphthalate) and calcium chloride were purchased from Fisher Chemical (Fair Lawn, NJ). Sodium chloride and hydrochloric acid were purchased from EM Science (Gibbstown, NJ).

Synthesis of Dextran Macromers. The synthesis of dextran macromers is shown in Figure 1a; a similar reaction has been reported previously.[26] To incorporate amine and carboxyl groups, dextran reacted with BEAHB and chloroacetic acid in the presence of triethylamine. An example of Dex-BH synthesis is given here. Predried dextran (2.0 g) was dissolved in anhydrous DMSO under nitrogen gas at room temperature. Triethylamine (11.2 mL) was then injected into the above solution. Meanwhile, BEAHB (7.5 g) was dissolved in DMSO and then added to the above solution dropwise, and stirred for 5 h at 50 °C. Dex-BH was then obtained by precipitating the filtered solution into excess cold isopropyl alcohol. The product was further purified three times by dissolution/precipitation with DMSO/cold isopropyl alcohol. The final product was dried overnight at room temperature under vacuum before further use. Dex-CA was synthesized similarly.

Self-Assembly of Tubular Structure. The rationale of this tubule self-assembly is to introduce oppositely charged carboxyl and amine groups, so that they could interact to self-assemble into tubular structures under appropriate condition. Dex-BH and Dex-CA were separately dissolved in buffer solutions (pH 4.0) at the concentration of 2.5 mg/mL, and they were then mixed and sonicated for 2 min in a sonicating water bath (Branson 3510R-DTH sonicator, Branson, Danbury, CT). The solutions were stored for at least 2 h at room temperature before any further test. All self-assemblies were formed at the same concentration.

Because protonation and deprotonation are pH dependent, the pH of the medium is expected to influence the extent of intermolecular interaction between Dex-BH and Dex-CA. In this study, a series of self-assemblies at different pH (3.0, 4.0, 5.0, and 7.0) medium is examined to determine pH effect. Since salt ions could also interact with both amine and carboxyl groups in the two precursors and hence change the intermolecular interaction between Dex-BH and Dex-CA, self-assembly at different salt concentrations is also investigated. The pH was kept at 4.0, and a NaCl solution with two different concentrations (0.01 and 0.03 M) was prepared. The self-assembly at different salt concentrations were prepared as previously described.

Self-Assembly Morphology. The morphology of the assemblies was studied by a scanning electron microscope (Leica Cambridge Stereoscan 440, Cambridge, UK) in both air-dried and freeze-dried mode. In the air-dried mode, the self-assembling solution was dropped onto the surface of the aluminum SEM stub and air-dried for 2 h; the dried samples were then gold sputter-coated (JFC-1200 Fine Coater, Japan) for 15 s. The SEM examination was conducted at 25 kV accelerating voltage and 12 nA probe current. In the freeze-dried mode, the solution was quickly frozen in liquid nitrogen and then freeze-dried in a Virtis Freeze Drier (Gardiner, NY) for 3 days at −50 °C under vacuum. The specimen was spread onto the aluminum SEM stub with double-sided carbon tape, and the specimen was gold-coated and observed as described above. This mode of preparation is expected to reveal self-assembled morphology in an aqueous state.

The morphology of the assemblies in an aqueous condition was also directly examined with a polarized light microscope (Olympus BX51, Tokyo, Japan). The solution was dropped onto the glass slide and covered with a glass coverslip; the sample slide was placed on the microscope stage. The image was monitored and recorded with enhanced measurement/archiving PAX-it software. In addition, a digitized image of a microruler was recorded for calibration.

X-ray Diffraction Study. To examine whether the assembly was driven by crystallization, a wide-angle X-ray diffractometer (WAXD, Scintag, Cuttertino, CA) was employed to obtain the X-ray diffraction patterns of the precursors and the self-assembly. The two precursors (Dex-CA and Dex-BH) were dissolved in a pH 4.0 hydrochloric acid solution; remaining procedures were the same as for self-assembly section. The assemblies were collected, placed in a tray, and then mounted onto the holder. In this study, the WAXD patterns were obtained under the condition of 45 KV and 40 mA with a continuous scan mode at the speed of 2.5°/min from 2° to 50°.

Dynamic Light Scattering (DLS) Study. Dynamic light scattering was performed with a DynaPro LSR (Proterion Corporation, Piscattaway, NJ). To investigate the assembly formation mechanism, 100 μL of the assembly solution at different time intervals was transferred into the testing cuvette and placed into the light scattering instrument. The experiment was measured at 25 °C with laser light wavelength of 826.2 nm at the angle of 90°, and the data was collected with the Dynamics program.

Acknowledgment. We are grateful for the financial support of the College of Human Ecology at Cornell University (assistantship to G. Sun), which made this study possible. We are also thankful to Sravanti Kusuma for proofreading this paper.

REFERENCES AND NOTES

1. Park, C.; Lee, I. H.; Lee, S.; Song, Y.; Rhue, M.; Kim, C. Cyclodextrin-Covered Organic Nanotubes Derived from Self-Assembly of Dendrons and Their Supramolecular Transformation. *Proc. Natl. Acad. Sci. U.S.A.* **2006**, *103*, 1199–1203.
2. Yan, D.; Zhou, Y.; Hou, J. Supramolecular Self-Assembly of Macroscopic Tubes. *Science* **2004**, *303*, 65–67.

3. Discher, D. E.; Eisenberg, A. Polymer Vesicles. *Science* **2002**, *297*, 967–973.
4. Van Tomme, S. R.; Mens, A.; van Nostrurn, C. F.; Hennink, W. E. Macroscopic Hydrogels by Self-Assembly of Oligolactate-Grafted Dextran Microspheres. *Biomacromolecules* **2008**, *9*, 158–165.
5. Rosler, A.; Vandermeulen, G. W. M.; Klok, H.-A. Advanced Drug Delivery Devices *via* Self-Assembly of Amphiphilic Block Copolymers. *Adv. Drug Delivery Rev.* **2001**, *53*, 95–108.
6. Kim, T.-i.; Seo, H. J.; Choi, J. S.; Jang, H.-S.; Baek, J.-u.; Kim, K.; Park, J.-S. PAMAM-PEG-PAMAM: Novel Triblock Copolymer as a Biocompatible and Efficient Gene Delivery Carrier. *Biomacromolecules* **2004**, *5*, 2487–2492.
7. Zhang, S.; Gelain, F.; Zhao, X. Designer Self-Assembling Peptide Nanofiber Scaffolds for 3D Tissue Cell Cultures. *Semin. Cancer Biol.* **2005**, *15*, 413–420.
8. Holmes, T. C.; de Lacalle, S.; Su, X.; Liu, G.; Rich, A.; Zhang, S. Extensive Neurite Outgrowth and Active Synapse Formation on Self-Assembling Peptide Scaffolds. *Proc. Natl. Acad. Sci. U.S.A.* **2000**, *97*, 6728–6733.
9. Das, R.; Kiley, P. J.; Segal, M.; Norville, J.; Yu, A. A.; Wang, L.; Trammell, S. A.; Reddick, L. E.; Kumar, R.; Stellacci, F.; et al. Integration of Photosynthetic Protein Molecular Complexes in Solid-State Electronic Devices. *Nano Lett.* **2004**, *4*, 1079–1083.
10. Selinger, J. V.; Schnur, J. M. Theory of Chiral Lipid Tubules. *Phys. Rev. Lett.* **1993**, *71*, 4091–4094.
11. Yang, W. Y.; Lee, E.; Lee, M. Tubular Organization with Coiled Ribbon from Amphiphilic Rigid-Flexible Macrocycle. *J. Am. Chem. Soc.* **2006**, *128*, 3484–3485.
12. Raez, J.; Manners, I.; Winnik, M. A. Nanotubes from the Self-Assembly of Asymmetric Crystalline−Coil Poly(ferrocenylsilane-siloxane) Block Copolymers. *J. Am. Chem. Soc.* **2002**, *124*, 10381–10395.
13. Santoso, S.; Hwang, W.; Hartman, H.; Zhang, S. Self-Assembly of Surfactant-like Peptides with Variable Glycine Tails to Form Nanotubes and Nanovesicles. *Nano Lett.* **2002**, *2*, 687–691.
14. Percec, V.; Dulcey, A. E.; Balagurusamy, V. S. K.; Miura, Y.; Smidrkal, J.; Peterca, M.; Nummelin, S.; Edlund, U.; Hudson, S. D.; Heiney, P. A.; *et al*. Self-Assembly of Amphiphilic Dendritic Dipeptides into Helical Pores. *Nature* **2004**, *430*, 764–768.
15. Zhang, S.; Marini, D. M.; Hwang, W.; Santoso, S. Design of Nanostructured Biological Materials Through Self-Assembly of Peptides and Proteins. *Curr. Opin. Chem. Biol.* **2002**, *6*, 865–871.
16. Yu, K.; Eisenberg, A. Bilayer Morphologies of Self-Assembled Crew-Cut Aggregates of Amphiphilic PS-b-PEO Diblock Copolymers in Solution. *Macromolecules* **1998**, *31*, 3509–3518.
17. Grumelard, J.; Taubert, A.; Meier, W. Soft Nanotubes from Amphiphilic ABA Triblock Macromonomers. *Chem. Commun.* **2004**, 1462–1463.
18. Ghadiri, M. R.; Granja, J. R.; Milligan, R. A.; McRee, D. E.; Khazanovich, N. Self-Assembling Organic Nanotubes Based on a Cyclic Peptide Architecture. *Nature* **1993**, *366*, 324–327.
19. Schnur, J. M.; Ratna, B. R.; Selinger, J. V.; Singh, A.; Jyothi, G.; Easwaran, K. R. K. Diacetylenic Lipid Tubules: Experimental Evidence for a Chiral Molecular Architecture. *Science* **1994**, *264*, 945–947.
20. Mitchell, J. C.; Harris, J. R.; Malo, J.; Bath, J.; Turberfield, A. J. Self-Assembly of Chiral DNA Nanotubes. *J. Am. Chem. Soc.* **2004**, *126*, 16342–16343.
21. Wong, G. C. L.; Tang, J. X.; Lin, A.; Li, Y.; Janmey, P. A.; Safinya, C. R. Hierarchical Self-Assembly of F-Actin and Cationic Lipid Complexes: Stacked Three-Layer Tubule Networks. *Science* **2000**, *288*, 2035–2039.
22. Zhang, Y. L.; Won, C. Y.; Chu, C. C. Synthesis and Characterization of Biodegradable Hydrophobic−Hydrophilic Hydrogel Networks with a Controlled Swelling Property. *J. Polym. Sci. Pol. Chem.* **2000**, *38*, 2392–2404.
23. Hu, Y.; Jiang, X.; Ding, Y.; Ge, H.; Yuan, Y.; Yang, C. Synthesis and Characterization of Chitosan-Poly(acrylic acid) Nanoparticles. *Biomaterials* **2002**, *23*, 3193–3201.
24. Matsui, H.; Gologan, B. Crystalline Glycylglycine Bolaamphiphile Tubules and Their pH-Sensitive Structural Transformation. *J. Phys. Chem. B* **2000**, *104*, 3383–3386.
25. Takahashi, N.; Kishimoto, T.; Nemoto, T.; Kadowaki, T.; Kasai, H. Fusion Pore Dynamics and Insulin Granule Exocytosis in the Pancreatic Islet. *Science* **2002**, *297*, 1349–1352.
26. Sun, G.; Chu, C.-C. Synthesis, Characterization of Biodegradable Dextran-Allyl Isocyanate-Ethylamine/Polyethylene Glycol-Diacrylate Hydrogels and Their *in Vitro* Release of Albumin. *Carbohydr. Polym.* **2006**, *65*, 273–287.